United Kingdom Atomic Energy Authority

RESEARCH GROUP

Preprint

ENERGY LOSS FROM A THETA PINCH

T. S. GREEN
D. L. FISHER
A. H. GABRIEL
F. J. MORGAN
A. A. NEWTON

Culham Laboratory
Abingdon Berkshire

1966

UNCLASSIFIED
(Approved for publication)

CLM - P 124

ENERGY LOSS FROM A THETA PINCH

by

T.S. GREEN
D.L. FISHER
A.H. GABRIEL
F.J. MORGAN
A.A. NEWTON

(Submitted for publication in Physics of Fluids)

A B S T R A C T

Electron temperatures measured in a megajoule theta pinch are found to be limited to ~ 300 eV over the pressure range 10-50 mtorr and to vary during the discharge time in a non-adiabatic manner. The plasma diamagnetism shows a rapid decay at the time of maximum Poynting flux and since there is no particle loss at this time there must be an energy loss of the order of the energy input rate.

Variation of the concentration of oxygen, which is the major impurity, by addition of known amounts or by reduction of the intrinsic 1.5% an order of magnitude with a new pre-ionization technique, indicates an energy loss rate of 2×10^{13} erg cm^{-3} sec^{-1} at zero oxygen concentration. It is not possible to account for this loss by radiation in the continuum spectrum.

A simple model of axial thermal conduction is developed in which the energy is transported to cold regions beyond the ends of the theta pinch coil. The model predicts a limiting temperature due to the steep temperature dependence of the conductivity coefficient $K = \alpha T^{5/2}$. Other predictions of the model concerning the variation of diamagnetism are found to be valid.

Finally the results of other theta pinch experiments are examined and some are found to fit the model.

U.K.A.E.A. Research Group,
Culham Laboratory,
Nr. Abingdon,
Berks.

September 1966 (ED)

CONTENTS

INTRODUCTION

In recent years the study of the characteristics of plasma produced in theta pinch devices has been extended to the investigation of containment of the plasma in coils of 100–200 cm length by the use of megajoule condenser bank facilities[1-5]. One conclusion derived from this data by the group in this laboratory[1] was that there was a loss of energy from the plasma other than the axial flow of particles out of the coil.

The evidence for energy loss was that the electron temperature reached its peak value at 3 μsec, and stayed nearly constant up to 6 μsec, even though the magnetic pressure was increasing and doing work on the plasma. The neutron yield also peaked during this time indicating that the ion energy had maximised earlier than peak magnetic compression. Measurements of plasma diamagnetism also lead to this conclusion since the diamagnetism, which is a measure of plasma energy, decreased more rapidly than predicted by adiabatic compression theory. This decrease, in particular, showed that energy was being lost from the mid-plane of the coil during the time 3–6 μsec. Independent measurements of particle containment showed that particles were not lost from the central plane prior to 6 μsec[6,7], so that the energy loss could not be due to axial convection.

Two possible explanations for this energy loss were radiation by impurity ions and conduction of the heat by the electrons. Spectroscopic observations indicated the presence of 1–3% O_2 in the discharge and strong line radiation from the OVII and OVIII ions. Simple estimates showed that the possible level of radiation energy was less than, but not too far removed from the energy loss. The alternative possibility of loss by thermal conduction along the magnetic field lines to the cold regions at the ends of the discharge coil has been discussed by Bickerton[8] who showed that this was the dominant axial energy transport mechanism when the ratio of the electron-electron mean free path to the coil length was less than unity but greater than the square root of the electron-ions mass ratio. The parameters of this experiment are such that this condition is satisfied. Calculations showed

that the rate of loss of energy by this process was also not too far different from the experimentally observed rate.

In order to estimate the relative importance of these processes we have carried out a further series of experiments which we report in the present paper. Firstly, we have investigated the effects of impurities on the rate of loss of energy and on the electron temperature attained. The impurity level has been increased by the addition of known quantities of oxygen and decreased to $0.15 \pm 0.1\%$ oxygen by the use of a new pre-ionization technique[9,10]. The results indicate that the level of radiation due to impurities is too low to explain the observed energy loss.

To investigate the effect of thermal conductivity we have made measurements with various parameters of the condenser bank and discharge coil. A simple theory of magnetic compression of a plasma which loses energy by thermal conduction shows that the temperature can only reach a value at which the rate of loss of energy equals the maximum rate of input of energy. This leads to a relationship between the maximum attainable temperature and the maximum rate of energy input. We have studied this relationship experimentally by varying the condenser bank energy.

The theory also shows that the rate of loss of energy varies as the inverse square of the coil length, a relationship which we have investigated by varying the length of the discharge coil.

The experimental data on scaling of the temperature and plasma diamagnetism agree well with the predictions of theory showing that the loss mechanism is a collision dominated diffusion process. However to fit the models describing the plasma behaviour we require the coefficient of thermal conductivity to be a factor of three greater than that calculated by transport theory[11].

Consequently we deduce that the dominant energy loss mechanism in the time of 3 to 6 μsec is thermal conduction and that this process limits the temperature attainable in our experiments. Comparison with similar experiments indicates that a limitation is observed when the plasma parameters are in the range given by Bickerton[8].

EXPERIMENTAL TECHNIQUES

The experiment was carried out using the Culham Megajoule Theta Pinch[1]. Deuterium gas at pressures of 10 mtorr to 100 mtorr was pre-ionized by a short duration pulse of axial current. The ionized gas was shock heated and compressed by the magnetic field generated by discharging the megajoule condenser bank through the 2 metre long, 10 cm diameter coil. Measured densities and temperatures during the compression were of the order of 10^{17} cm^{-3} and 300 eV.

In the present experiment some temperature determinations were made using the soft x-ray foil absorption technique[12]. A double pin-hole camera assembly recorded the transmission through two different foils simultaneously. Normally beryllium foils of 21.6 and 43.2 mg cm^{-2} were used, since the ratio of transmitted intensity for these foils gives a sensitive function of temperature in the range 200-400 eV.

The plasma diamagnetism was measured at planes along the coil length from the centre to the end at 25 cm separation, using the technique of balanced probes[13] in which the total flux through the coil is compared with the magnetic field strength.

Spectroscopic observations in the visible and quartz ultra-violet were made using a monochromator viewing the plasma radially through the quartz discharge tube. This observation was made to determine the concentration of impurities in the discharge.

A two metre grazing incidence photographic spectrograph[14] was used to record the spectrum in the far ultra-violet in the range down to 5 Å. Time resolution was achieved by means of a fast mechanical shutter capable of use down to 1 μsec[15]. Absolute calibration of the instrument was carried out independently[16] over the wavelength range 10-100 Å, allowing the instrument to be used for absolute measurements of the level of radiated energy.

EXPERIMENTAL RESULTS

SPECTROSCOPIC MEASUREMENTS

The spectroscopic observations in the far ultra-violet show both a strong continuum and a number of lines. These two features can be considered separately as they have different sources.

(a) Line Spectrum

The line spectra indicate the chief impurity as oxygen, and to a lesser extent in descending order of concentration, silicon, carbon, chlorine and sulphur. Oxygen is noticeably the strongest impurity radiation and its ionization life-history can be followed through the discharge. From 2 to 8 μsec it is present as OVII and OVIII with OVIII dominating by a small factor of two or three towards the end of the half-cycle. Throughout this period, the chief source of radiation is the resonance lines of these two ions. Interpretation of the observed intensities of these lines was thought inadvisable, since approximate calculations indicated a large optical depth in the axial direction. However, their observed intensities were found in practice to be a function of oxygen concentration, so that alignment discrepancies and parallax effects must have been causing a considerable reduction in the optical depth along the viewing direction.

The actual oxygen concentration was determined by observing lines of OII and OIII by radial observation in the visible and quartz U.V. region using a monochromator. These lines were observed during the early phase of the discharge. Their intensity was measured as a function of added oxygen concentration. Extrapolation back to zero added oxygen indicated a residual impurity level of $1.5\% \pm 0.5\%$ of oxygen.

(b) Continuum Spectrum

The grazing incidence spectra exhibited a continuum at short wavelengths with a maximum in the region of 30 Å. Such a continuum can arise from free-free and free-bound radiation from the deuterium and the impurity ions. The hydrogenic

approximation for this radiation, which becomes increasingly valid as the charge on the ion increases, predicts the same wavelength dependence of the radiation for both types of radiation and for all ions, provided the free-bound discontinuities do not occur in the wavelength range of interest. This dependence is given by

$$E_\lambda \propto \frac{1}{\lambda^2} \exp\ (-\ 12{,}400/\lambda T) \qquad \ldots\ (1)$$

for T in eV and λ in Å, if one takes the Gaunt factor to be unity.

Such a spectrum has a maximum intensity at a wavelength λ_m given by

$$\lambda_m = \frac{6200}{T} \qquad \ldots\ (2)$$

Consequently it is possible to determine the electron temperature from the wavelength of maximum intensity after correcting the spectrum for the instrument sensitivity and dispersion.

Values of T_e determined in this way are shown in Table 1, together with the effect of added impurity, pressure and capacitor bank energy.

TABLE 1

ELECTRON TEMPERATURES MEASURED WITH THE GRAZING INCIDENCE SPECTROGRAPH

Pressure (mtorr)	$\frac{\omega \hat{B}^2}{8\pi}$ (erg cm^{-3} sec^{-1})	Oxygen Impurity	Exposure Time Interval (μsec)	T_e (eV)
20	4.0×10^{13}	1.5%	0–2	208 ± 60
20	4.0×10^{13}	1.5%	2–4	250 ± 25
20	4.0×10^{13}	1.5%	4–6	240 ± 24
20	4.0×10^{13}	1.5%	6–8	235 ± 24
20	4.0×10^{13}	1.5%	2–10	247 ± 25
20	1.6×10^{13}	–	2–10	180 ± 18
20	1.0×10^{13}	–	2–10	143 ± 15
20	0.5×10^{13}	–	2–10	126 ± 18
20	4.0×10^{13}	0.15%	2–10	248 ± 40
20	4.0×10^{13}	3.5%	2–10	240 ± 24
10	4.0×10^{13}	–	2–10	229 ± 23
30	4.0×10^{13}	–	2–10	232 ± 23

From the calibration of instrument sensitivity it was also possible to determine the total energy radiated in the continuum. Under typical conditions of 20 μ D_2 it was ~ 7×10^{11} ergs cm^{-3} sec^{-1}, and varied by factors of two or three for experimental runs taken at different times, but was not correlated with the level of oxygen impurity.

The level of continuum is also higher than can be calculated on the basis of free-free and free-bound continuum for the OVII and OVIII ions. The continuum level for 1% O_2 in a plasma of 300 eV electron temperature and 10^{17} cm^{-3} electron density, amounts to a total of 2×10^{10} ergs cm^{-3} sec^{-1}. This is slightly below the amount for the deuterium free-free continuum.

An additional impurity must be present to account for the higher level of the measured continuum intensity. Since there are neither obvious recombination discontinuities nor line spectra correlating with the continuum intensity in the region below 100 Å, it is necessary to discount the impurities mentioned in (a) above and look for a heavier element. A heavier element will ionize to produce both a higher resultant charge and a lower final ionization potential, and both these effects will tend to produce the observed spectrum. Moreover, only a small concentration would be required. A test with krypton added showed this to be far too light. However, an addition of ~ 0.1% of mercury had the effect of increasing the observed continuum without either introducing new lines, or measurably changing the electron temperature. Since mercury from the diffusion pumps is a possible contaminant, it was concluded that a residual concentration of < 0.1% was responsible for the continuum observed.

SOFT X-RAY MEASUREMENTS

Mean values of temperature determinations made using this technique are plotted as a function of time in Fig. 1 for an initial pressure of 30 mtorr. The maximum value of 310 ± 40 eV was attained in 5 μsec, although the variation from 2.5 to 7 μsec was small, being less than 10%.

Temperature measurements were made over a range of pressures using this technique. The maximum value of temperature obtained at each pressure is plotted against pressure in Fig.2.

PLASMA DIAMAGNETISM

(a) Typical Data

A set of data for the variation of the plasma diamagnetism with time at various positions along the length of the coil is shown in Fig.3. Also shown is a curve computed for the adiabatic compression of a loss-less plasma. The relative decrease of the experimental signals below the computed curve we ascribe to energy loss (see Discussion and Appendix). Near the coil ends this is primarily axial convection - or flow of particles. Near the centre the decrease occurs before the rarefaction wave of axial loss[17,18] has reached the centre. Consequently the diamagnetic signal in the central plane is a good diagnostic for the loss process in the first six microseconds (under different conditions this time varies but it is still true that there is a period of several microseconds before the central data are perturbed by particle losses - this perturbation usually shows up quite clearly as will be seen later).

(b) Measurements with Added Impurities

We have measured the diamagnetism of the plasma containing known quantities of oxygen impurity. These were added by expanding a small known volume of oxygen at a measured high pressure into the known large volume of the discharge tube. Since it has been thought that the oxygen can be adsorbed on the tube walls so leading to erroneous results, we monitored the amount of oxygen in two ways.

The first was a relative measurement in which the intensities of the OII and OIII line radiations were determined as described above. These measurements showed that the intensity of oxygen line radiation from the plasma increased linearly with the amount of gas added. The second measurement was of the plasma line mass as determined from the frequency of the hydromagnetic radial oscillations

excited by the pinch[19]. Changes in the line mass could be measured to within 40% and showed that, within experimental error, the contaminant gas was all trapped in the plasma.

A set of diamagnetic signals for various amounts of added oxygen are shown in Fig.4. To turn these into a more quantitative measure of the effect of impurities on energy loss we have determined the loss rate from the shape of the diamagnetic signal between 3 and 5 μsec from equation (A7) with $\varphi = 0$ (see Appendix). Results are shown in Fig.5.

In the normal range of experiments performed the minimum attainable level of impurity was 1.5 ± 0.5%. With the large errors in determination of energy loss rate and oxygen content, it was difficult to be certain of the loss rate at zero oxygen content. To overcome this difficulty we have used a new pre-ionization system, similar to that originated at Garching[10], generating a very short pulse of current to ionize the gas. This system has limitations in efficiency of ionization and subsequent shock heating of the gas, but is capable of producing a much purer plasma by starting the main pinch before the pre-ionized plasma has expanded to the tube walls[9]. We have obtained low impurity levels ~ 0.15 ± 0.1% and this has enabled us to estimate the energy loss rate at zero oxygen content with higher accuracy.

At the same time the electron temperature was checked with the grazing incidence spectrograph and found to be the same as in the normal range of experiments (see Table I).

(c) Variation of Coil Length

We have also used the plasma diamagnetism as a monitor of the effect of varying the coil length. The effective length of the coil was changed by removing a section of the coil. The whole coil consisted of eight sections each 25 cm long, so that by removing one of them we could produce coils of any effective length. This procedure minimised the change in inductance and therefore voltage in the coil. Consequently we assume that, to a first approximation, the initial stages

of the pinch are unchanged and the parameters of the plasma after 1 μsec are independent of coil length. This is confirmed by the negligible change in the plasma diamagnetism at 1 μsec produced by the removal of one coil section.

Only a few curves were obtained, at pressures of 43 and 61 mtorr (Fig.6). At lower pressures there were indications of instabilities when using the shorter coils. The experiment was terminated by a failure of the discharge tube and burning of the coils.

DISCUSSION

RELATION BETWEEN TEMPERATURE AND DIAMAGNETISM

The two plasma parameters which we have measured in these experiments are the electron temperature and the diamagnetism. It was not always possible to measure both parameters in each phase of the experiment. Further the temperature measurement is an average taken axially whilst the diamagnetism is measured in different axial planes. Sometimes therefore we have to consider the analysis of the data in terms of temperature and sometimes in terms of diamagnetism.

It is important to note, however, that there is a relation between the two quantities which enables us to correlate the separate analyses. To see this relation, consider the simplest model for the plasma, one of uniform temperature and density with no trapped flux, with equal and isotropic ion and electron temperature. It then follows (see Appendix) that

$$S = A.B \quad - \quad \text{definition of diamagnetic signal}$$

$$2nkT = \frac{B^2}{8\pi} \quad - \quad \text{pressure balance}$$

$$nA = N \quad - \quad \text{definition of line density}$$

Hence

$$T = \frac{BS}{16\pi Nk}$$

Allowing for trapped flux in the plasma $S = A.B - \varphi$ and

$$T = \frac{BS}{16\pi Nk}\,(1 + \varphi/(S + \varphi)) \qquad \ldots (3)$$

EVIDENCE FOR ENERGY LOSS

The main evidence for energy loss is the time history of both temperature and plasma diamagnetism. It can be seen from Fig. 1 that the electron temperature is essentially constant from 2.5 to 7 μsec even when the magnetic field strength is increasing and doing work on the plasma. This indicates an energy loss.

To express this analytically, the simple model for the plasma, which we shall use in discussing the data (see Appendix), shows that the magnetic compression of a plasma without energy loss should increase the temperature according to the relation

$$\frac{1}{T}\frac{dT}{dt} = \frac{4}{6-\beta}\frac{1}{B}\frac{dB}{dt} \qquad \ldots (4)$$

If there is an energy loss, then

$$\frac{1}{T}\frac{dT}{dt} = \frac{4}{6-\beta}\cdot\frac{1}{B}\frac{dB}{dt} - \frac{R}{B^2}\cdot 16\pi\frac{(2-\beta)}{(6-\beta)} \qquad \ldots (5)$$

Consequently the observation that $\frac{dT}{dt}$ is zero when $\frac{dB}{dt}$ is finite signifies an energy loss rate, R, of the order of $\omega\frac{\hat{B}^2}{16\pi}$ i.e. in our case 4×10^{13} ergs $cm^{-3}sec^{-1}$.

It follows from the relationship between the diamagnetism S and temperature T, that the time history of S should also reflect the energy loss. In fact, analysis using this simple model for the plasma shows that the variation of diamagnetism is given by the equation

$$\frac{1}{S}\frac{dS}{dt} = -\frac{1}{B}\frac{dB}{dt}\left[\frac{1+\varphi^2/(S+\varphi)^2}{5+\varphi^2/(S+\varphi)^2}\right] - \frac{16\pi R}{B^2[5+\varphi^2/(S+\varphi)^2]} \qquad \ldots (6)$$

From this equation we calculate that the mean rate of loss of energy from the plasma during the time 3 to 5 μsec is 2.5×10^{13} ergs cm^{-3} sec^{-1}.

RADIATION

The main features of the ultra-violet spectrum are, as discussed above, the broad continuum due to highly stripped heavy ions, and the oxygen line radiation of OVII and OVIII.

The total energy in the continuum is measured to be 7×10^{11} ergs cm^{-3} sec^{-1} and is too low by two orders of magnitude to explain the energy loss from the plasma.

The energy in the oxygen line spectrum cannot be determined experimentally since in the viewing solid angle the lines may be optically thick; hence one can only estimate their contributions to energy loss. Oxygen at these densities and temperatures is assumed to be in coronal-type excitation equilibrium, so that the ions are excited by electron impact and lose energy by radiation. The energy radiated is then the product of the excitation rate and the photon energy summed over all resonance lines. The excitation rate coefficient of a level of energy W eV in a plasma of temperature T eV is approximately given by

$$S = 3 \times 10^{-6} \frac{f}{T^{\frac{1}{2}} W} e^{-W/T} \text{ cm}^3 \text{ sec}^{-1} \qquad \ldots (7)$$

where f is the oscillator strength for the equivalent optical transition[20]. Hence

$$E = 3 \times 10^{-6} \frac{N_q N_e}{T^{\frac{1}{2}} W} h\nu \; e^{-W/T} \text{ ergs cm}^{-3} \text{ sec}^{-1}$$

where N_q and N_e are the ion and electron densities and W is now the energy of the strongest resonance line. f has been taken to be unity, this overestimate compensating to some extent for the approximation of taking only the strongest resonance line. Since $\frac{h\nu}{W}$ is clearly just 1.6×10^{-12} ergs eV^{-1}, this can be written

$$E = 5 \times 10^{-18} \frac{N_q N_e}{T^{\frac{1}{2}}} \cdot e^{-W/T} \text{ ergs cm}^{-3} \text{ sec}^{-1} \qquad \ldots (8)$$

The problem of determining how much of the oxygen is in an ion stage q is simplified in the present case by the observation that for all times of interest OVII and OVIII are the dominant ions. Since W is almost the same for these two ions (570 eV and 650 eV respectively), the two can be treated as one ion with W = 600 eV and N equal to the oxygen density. Values of T = 300 eV, $N_e = 10^{17}$, $N_i = 10^{15}$ then give $E = 4 \times 10^{12}$ ergs cm^{-3} sec^{-1} as the estimated total line radiation from 1% oxygen impurity.

This is significantly lower than the observed energy loss and even the large uncertainties in the cross sections are unlikely to account for this difference. However, there is also the experimental observations of the effect of impurities

on the plasma diamagnetism. These data have been used to determine the variation of the rate of energy loss R from the plasma with impurity content using equation (A7) (Fig.5).

We assume that, to a first approximation, the effect of added oxygen is a linear one, i.e. that

$$R = R_0 + R^1 O \qquad \ldots (9)$$

where R_0 is the loss rate from an oxygen free plasma and R^1 is the loss rate produced by 1% of added oxygen, O being the percentage of added oxygen. By fitting such a line to the data we find that R^1 is equal to $3.5 \pm 2 \times 10^{12}$ in close agreement with the value estimated above, and that R_0 is equal to $2.0 \pm 0.5 \times 10^{13}$ ergs cm^{-3} sec^{-1}.

ENERGY LOSS BY THERMAL CONDUCTION

(a) Computations

To discuss the effect of thermal conduction on the behaviour of the plasma it is necessary to create a model of the plasma compression by the magnetic field, which takes into account an energy loss term equal to $\frac{\partial}{\partial z}\left(K \frac{\partial T}{\partial z}\right)$. [K is the coefficient of thermal conductivity which for a plasma can be written as $\alpha T^{5/2}$ (11).]

One approach is to set up the two fluid magnetohydrodynamic equations including the loss term and solve them by computation. In principle, this can be done using a two-dimensional form of the magnetohydrodynamic code developed for theta pinches[21]. However, this code has not yet reached a sufficiently advanced stage for a direct application to this problem. Consequently we resort to several different approximations.

(i) Uniform one fluid plasma

The simplest model for the plasma, is to assume that it is radially uniform in properties; i.e. both temperature and density are independent of radius. A second assumption is to make the electron and ion temperatures equal and isotropic; this simplifies calculations but does not alter many of

the predictions of the theory. In such a plasma the area and trapped magnetic flux can be specified uniquely. Then the equation of energy balance for one centimetre length of plasma can be written quite simply and used as a basis for calculating the behaviour of the magnetic compression.

It is necessary, however, to make further assumptions in order to evaluate the term $\frac{\partial}{\partial z}\left(K \frac{\partial T}{\partial z}\right)$. We assume that the dominant process determining $\frac{\partial T}{\partial z}$ is thermal conduction and completely neglect the effect of axial flow on the properties not only in the central plane, which is justifiable, but also at other points along the plasma. Making this assumption it is reasonable also to say that T is an independent function of z and time. Then it is possible to reduce the equation for energy balance to one for the time variation of temperature and also of plasma diamagnetism (see Appendix).

$$\frac{1}{T_c}\frac{dT_c}{dt} = \frac{4}{(6-\beta)} \cdot \frac{1}{B}\frac{dB}{dt} - \frac{0.47 \cdot 16\pi a\ (2-\beta)}{B^2 L^2\ (6-\beta)} \cdot T_c^{7/2} \qquad \ldots (10)$$

$$\frac{1}{S}\frac{dS}{dt}\left[1 + \frac{1}{5}\left(\frac{\varphi}{S+\varphi}\right)^2\right] = -\frac{1}{5}\frac{1}{B}\frac{dB}{dt}\left(1 + \frac{\varphi}{S+\varphi}\right)$$

$$- \frac{0.47 \times 16\pi a}{5L^2}\frac{B^{3/2}\ S^{5/2}}{(16\pi\ Nk)}\ 7/2\ (S+\varphi)\left(1 + \frac{\varphi}{S+\varphi}\right)^{7/2} \qquad \ldots (11)$$

(ii) <u>One dimensional (r,t) computation code</u>

A more accurate computation should be to use the radial one-dimensional magnetohydrodynamic computation code inserting an energy loss term. Again the problem arises of axial variation of T and computation of the derivative with respect to z. We use the axial dependence calculated from the equations describing model (i).

(iii) <u>One dimensional (z,t) computation code</u>

Another approach is to use the radially uniform model of the plasma but allow for axial variations by writing in the axial dependence of all the terms in the magnetohydrodynamic equation. This approach has been used to investigate problems of axial flow of the plasma[18]. It is a simple modification to introduce the heat flow term and calculate the temporal behaviour of plasma parameters. However, the major difficulty which arises is that of introducing a heat sink with the proper boundary conditions.

The advantage of using model (i) is that the solution of equation (10) describes certain phenomena having a simple physical interpretation. The two computation codes serve to indicate limits to the details of interpretation.

The predictions of the models will be discussed and compared with experiment in the following sections.

(b) Temperature Limitation

It is possible to solve equation (10) for the time dependence of electron temperature taking an initial value for the temperature at 1 μsec, just after the shock heating phase. Results are shown in Fig.7 for the magnetic field parameters of our experiment. The striking feature of this calculation is that as the initial temperature is increased from 100eV the subsequent behaviour becomes less like that of an adiabatic compression, and the temperature starts to limit. In fact the results show that it is not possible to maintain a temperature above 350 V. This phenomenon we call temperature-limitation.

It is clear from equation (10) that the limitation arises because $\frac{\partial T}{\partial t}$ becomes negative when T exceeds a value given by

$$T^{7/2} = B \frac{\partial B}{\partial t} \frac{L^2}{0.47 \cdot 2\pi(2 - \beta)\alpha} \qquad \ldots (12)$$

Since $\frac{B\partial B}{\partial t}$ has a maximum at one eighth of the oscillation period of the circuit it follows that T has a maximum value given by

$$T_m^{7/2} = \frac{\omega \hat{B}^2 L^2}{4\pi\alpha \cdot 0.47 \cdot (2 - \beta).} \qquad \ldots (13)$$

when the rate of loss of energy by conduction is equal to the maximum rate of input of energy.

A similar limitation is shown by results of the (r,t) code when T_e is computed at different pressures. Lowering the pressure produces higher temperatures at the end of the shock phase and should, after magnetic compression, lead to higher maximum values for the temperature. Calculations involving thermal conduction loss show that this does not happen but that the temperature reaches a

limiting value (Figs.2 and 8). This agrees with the experimental observations that reducing initial pressure from 50 mtorr to 10 mtorr produces no significant change in temperature (Fig.2).

(c) Time History of Temperature

At pressures corresponding to this limited temperature, the compression is almost isothermal from 2.5 to 6 μsec. Both models (i) and (ii) predict this essentially because of the rapid variation of energy loss with temperature (Figs.7 and 8).

(d) Time History of Diamagnetism

Since the temperature and the diamagnetism are simply related as shown above, it is possible to fit the model to the data for the time variation of diamagnetism. This can be compared with the predictions of the (z,t) code and is shown for the mid-plane in Fig.9. In principle the relative importance of particle and heat flow can be studied with the axial variation of S. As shown by Wesson[18] the particle flow takes the form of a rarefaction wave propagating into the coil from the end at a velocity depending on the trapped flux in the plasma. In fitting the data therefore, both the trapped flux and the coefficient of thermal conductivity are varied.

From the comparison of theory and experiment thermal conduction dominates in the mid-plane up to 6 μsec. Near the ends of the plasma where the axial flow is of importance the choice of trapped flux is more critical as are the boundary conditions describing the temperature and location of the heat sink.

(e) Temperature Scaling Law with Power Input

The features discussed above are indicative only of an energy loss which increases rapidly with temperature. To determine the power dependence we have investigated the variation of T_e with rate of input of energy predicted by equation (13).

The experimental data quoted in Table I and plotted in Fig.10 fit a line

$$a \log T = \log (\hat{\omega} B^2) + b \qquad \ldots (14)$$

where

$$a = 3.3 \pm 0.8$$

which is to be compared with the theroetical value of 3.5 for the temperature index.

(f) Scaling Law with Length

Equation (10) predicts that T should scale with the coil length since the process is a diffusion of energy. Correspondingly the time variation of S should depend on L. Therefore we have compared the data on diamagnetism with the computations using equation (11).

First the measured temperatures are used to assign a value of φ for the particular pressures investigated. Then at the lowest pressure in the longest coil a value is selected for α to give the best fit with the experimental diamagnetism. All other cases are then computed using the value of φ appropriate to the pressure and modifying the equation only for the pressure and length variation. Experimental and computed curves are shown in Fig.6.

(g) The Absolute Value of Thermal Construction Coefficient

Estimates of the coefficient, α, of thermal conduction have been made in two ways: firstly, by comparison of the limiting temperature observed experimentally with the theoretical prediction (equation (13)) and secondly, by fitting equation (11) to the data on diamagnetic signals.

(i) From Limiting Temperature

The conduction coefficient is determined from equation (13) transformed to

$$\alpha = \frac{\omega \hat{B}^2 L^2}{4\pi \, 0.47 \, (2 - \beta)} \; \frac{1}{\hat{T}_m^{7/2}} \qquad \ldots (15)$$

In this case $\hat{T}_m$ is the limiting temperature in the central plane. The experimentally observed temperature T_e is however a mean value over the length of the plasma and is therefore different. The ratio of the two temperatures $T_e/T_m = \xi$ can be estimated assuming a certain axial variation of temperature and calculating the energy received by the detector allowing for solid angle effects and instrumental efficiency.

The estimate has been made for the axial variation of temperature assumed in the simple model for the plasma (see (a)(i) above and Appendix) as well as for variations obtained by computation with the (z,t) code.

In the case of the absorber foil technique, it is found that $\xi = 1.05 \pm 0.05$ covers all distributions studied: it is close to unity essentially due to the higher sensitivity to regions of higher temperature.

The value of ξ for the measurements made with the grazing incidence technique is higher $1.20 \pm .05$. Correction for the different values of ξ brings the temperatures observed by the two methods into closer agreement.

Inserting these corrected temperatures into equation (15) one obtains a value for α of $6 \pm 3 \times 10^{-6}$ ergs cm^{-3} sec^{-1} $^{o}K^{-7/2}$. The large error is due to the uncertainty in the temperature raised to a high power.

(ii) Diamagnetic Signals

We have fitted the experimental data on plasma diamagnetism using the three computational models outlined in (a) above. Since each involves certain different simplifying assumptions, different values of α have been required to obtain a good it to the data. The range of values used has been between 4×10^{-6} and 7×10^{-6} ergs cm^{-3} sec^{-1} $^{o}K^{-7/2}$ in agreement with the value quoted above.

These values we have obtained are to be compared with a value of 1.85×10^{-6} ergs cm^{-3} sec^{-1} $^{o}K^{-7/2}$ predicted from transport theory[11]. There have been no reported experimental determinations of α for a hot hydrogen plasma.

APPLICABILITY OF THEORY OF THERMAL CONDUCTION

It was pointed out by Bickerton[8] that there are different possible mechanisms for transport of energy axially from a theta pinch: mass flow of ions and electrons, diffusive loss of heat by electrons and loss of heat by free-streaming of the electrons.

The time constant for mass flow is of the order of the length divided by the ion velocity (L/v_i); that for heat diffusion of the order of the square of the coil length divided by the product of the electron velocity and the electron-electron mean free path $\left(\frac{L}{\lambda}\cdot\frac{L}{v_e}\right)$. Consequently the diffusion is the dominant energy transport mechanism provided

$$\frac{L}{\lambda}\cdot\frac{L}{v_e} < \frac{L}{v_i}$$

or

$$\frac{\lambda}{L} > \left(\frac{v_i}{v_e}\right) = \left(\frac{m_e T_i}{m_i T_e}\right)^{\frac{1}{2}} \qquad \ldots (16)$$

This limit is somewhat lower in practice since the containment time is longer than L/v_i depending on the β value of the plasma[18].

If $\frac{\lambda}{L}$ is greater than unity, the diffusion containment time is calculated to be less than the streaming time of the electrons, clearly physically impossible. The whole concept of diffusion must change as λ approaches L so that the theory applies only to the region

$$\frac{\lambda}{L} < 1 \qquad \ldots (17)$$

Above this limit, the containment time will depend on the conditions at the ends of the coil. The streaming electrons can create electric fields which inhibit their escape[22]. They can also be reflected by magnetic mirrors, so that the containment time becomes of order $\frac{\lambda}{v_e}$, and increases with increasing temperature.

The range of parameters obtained in our experiments is such that $\lambda/L \approx 0.02$ so that the theory is applicable. The value for λ has been calculated from the equation

$$\lambda = \frac{2\times 10^{13}}{\text{Log }\Lambda}\,\frac{T^2}{n}\ \text{cm, eV} \qquad \ldots (18)$$

and is consistent with the value of α given by transport theory.

COMPARISON WITH OTHER EXPERIMENTS

Early experiments on Theta Pinch devices were mainly concerned with the effects of reversed bias magnetic field in which axial flow of heat was inhibited

by closure of the field lines. In more recent experiments no bias magnetic field has been used and the axial flow of heat along the lines has to be considered.

Measurements of the electron temperature have been made over a wide range of pressures on the Scylla Machine[24]. The temperature was found to be constant with pressure from 10 to 125 mtorr and to vary non-adiabatically with time. Both observations are consistent with our model.

Electron temperatures are also available from the megajoule machines at Jülich[27] working at 50 mtorr and in low pressure regimes at General Electric[23] and Garching[26]. The relevant data are compared in Table 2 where it can be seen that the observations agree quite well with the predictions of equation (13) using the experimental value of α. However for the General Electric group the measured temperature is greater than we would predict and the relatively high value of λ/L may be significant in this case.

TABLE 2

Results of Megajoule Theta-pinch Experiments

	$\frac{\omega \hat{B}^2}{8\pi}$ erg cm^{-3} sec^{-1}	Coil half length L cm	$\frac{\lambda}{L}$	Electron Predicted eV	Temperature Measured eV
Los Alamos Scylla	15×10^{13}	50	0.03–0.16	295	295–330
Jülich	4.7	60		245	~200
Garching Isar	20	75	~0.1	425	420 ± 50*
General Electric	1.6	30	0.25	100	260

* Result from Thomson Scattering of ruby laser light

CONCLUSION

The experimental data show that the plasma loses energy at a rate of 2.5×10^{13} ergs cm^{-3} sec^{-1} during the time 3 to 6 μsec, before axial flow is important in the mid-plane of the coil.

The energy radiated by the dominant impurities has been shown to account for only 20% of this amount and is therefore insufficient to explain the observations.

If one calculates the loss rate due to thermal conduction using a theoretical coefficient then it also is too low to explain the observations at our temperatures. However, we have considered this possibility further and have found that a simple theory of compression of the plasma including heat loss by thermal conduction, leads to several predictions each of which is found to be experimentally valid:-

(i) the temperature will limit at a value over a range of starting pressures;

(ii) this limiting temperature is predicted to vary as the two sevenths power of the maximum rate of input of magnetic energy from the capacitor bank ($\omega \hat{B}^2$);

(iii) this limiting temperature and the rate of loss of energy are predicted to depend on the square of the coil length.

Furthermore it is possible, by choosing a value for the coefficient of the thermal conductivity greater than that given by transport theory, to obtain good quantitative agreement between theory and experiment over a wide range of operating parameters. Consequently we conclude that thermal conduction is the dominant energy loss mechanism in our experiments and with a coefficient of conduction some three times greater than the theoretical value.

The observations of other groups are also consistent with this theory for a variation of coil length of about a factor two and of power input of a factor of ten.

The theory is not valid in the limit when the collision mean free path becomes comparable to the coil length, a condition approached in one low density short coil experiment. The energy containment time is not necessarily increased by

working in this limit unless the electrons can also be contained. If mirror fields are applied then the containment time becomes λ/v_e and so increases rapidly with temperature as is known in mirror machines.

Experiments are now proceeding in this laboratory to investigate the containment of energy and particles in this limit.

ACKNOWLEDGEMENTS

The authors are grateful for many helpful discussions with Drs P.C. Thonemann, K.V. Roberts and G.B.F. Niblett, and many colleagues in the Culham Laboratory. We are also grateful to T. Quayle and his staff for the operation of the Megajoule facility and to G.C. Heywood and M.W. Alcock for assistance with the experiment.

REFERENCES

1. BODIN, H.A.B., and others. Plasma containment and stability in a megajoule theta pinch experiment. I.A.E.A. Conference on Plasma Physics and Controlled Nuclear Fusion Research, Culham, September 1965. Proceedings, vol.1, pp.193-221.

2. QUINN, W.E., and others. Stability, heating and end loss of a 3.5 MJ theta pinch (Scylla IV). I.A.E.A. Conference on Plasma Physics and Controlled Nuclear Fusion Research, Culham, September 1965. Proceedings, vol.1, pp.237-247.

3. ANDELFINGER, C., and others. Isar I - a fast megajoule theta pinch experiment with extremely high compression fields. I.A.E.A. Conference on Plasma Physics and Controlled Nuclear Fusion Research, Culham, September 1965. Proceedings, vol.1, pp.249-260.

4. BINGHAM, R.L., GOLDMAN, L.M., and KILB, R.W. Energy distribution of particles leaving a theta pinch. I.A.E.A. Conference on Plasma Physics and Controlled Nuclear Fusion Research, Culham, September 1965. Proceedings, vol.1, pp.301-313.

5. KOLB, A.C., and others. Plasma confinement, heating and losses in Pharos with an extended current pulse. I.A.E.A. Conference on Plasma Physics and Controlled Nuclear Fusion Research, Culham, September 1965. Proceedings, vol.1, pp.261-274.

6. DANCY, D.J. and KEILHACKER, M. Time resolved measurements of the radial density distribution in a theta pinch. Culham Laboratory, August 1965, CLM -M 55.

7. HILL, E.T., SEGRE, S.E. To be published.

8. BICKERTON, R.J. Simple theory of the compression cusp. Culham Laboratory, May 1964, CLM -M 35.

9. NEWTON, A.A. Fast high voltage Z-pre-ionization of a megajoule theta pinch. Culham Laboratory, July 1966, H.M.S.O. CLM -R 62.

10. ANDELFINGER, A. and others. Influence of impurities on the electron temperature in a theta pinch. Phys. Letters, vol.20, no.5, 15 March, 1966. pp.491-493.

11. SPITZER, L. The physics of fully ionized gases. 2nd ed. Interscience 1962.

12. PEACOCK, N.J. Soft x-ray emission from thetatron. Culham Laboratory, November, 1964. CLM -M 39.

13. GREEN, T.S. An investigation of the theta pinch using magnetic pick-up loops. Nucl. Fusion, vol.2, 1962. pp.92-101.

14. GABRIEL, A.H., SWAIN, J.R., and WALLER, W.A. A two-metre grazing-incidence spectrometer for use in the range 5 - 950 Å. Sci. Instrum., vol.42, no.2, February, 1965. pp.94-97.

15. FAWCETT, B.C. and GABRIEL, A.H. Spectra from $3p^n - 3p^{n-1}$ 3d transitions of the non period elements in the chlorine I and sulphur I isoelectronic sequences. Proc. Phys. Soc., vol.88, no.559, May, 1966. pp.262-264.

16. MORGAN, F.J., BARTON, M.J., and GABRIEL, A.H. Culham Laboratory. (To be published)

17. TAYLOR, J.B., and WESSON, J.A. End losses from a theta pinch. Nucl.Fusion, vol.5, no.2, June, 1965. pp.159-161.

18. WESSON, J.A. Plasma flow in a theta pinch. I.A.E.A. Conference on Plasma Physics and Controlled Fusion Research, Culham, September 1965. Proceedings, vol.1, pp.223-235.

19. GREEN, T.S., NIBLETT, G.B.F. Radial hydromagnetic oscillations. Proc. Phys. Soc., vol.74, no.6, December 1959. pp.737-743.

20. ALLEN, C.W. Astrophysical quantities. 2nd ed. Univ. of London, Athlone Press, 1963, p.42.

21. HAIN, K. and others. Fully ionized pinch collapse. Z. fur Naturf., vol.15a, no.12, 1960. pp.1039-1050.

22. HOBBS, G.D. and WESSON, J.A. Heat transmission through a Langmuir sheath in the presence of electron emission. Culham Laboratory, June 1966. H.M.S.O. CLM-R 61.

23. GOLDMAN, L.M. and others. Low-density theta pinch experiments. Phys. Fluids, vol.8, no.3, March 1965, pp.522-528.

24. LITTLE, E.M., QUINN, W.S. and SAWYER, G.A. Plasma end losses and heating in the "low pressure" regime of a theta pinch. Phys. Fluids, vol.8, no.6, June, 1965. pp.1168-1175.

25. HAAS, F.A. Culham Laboratory. Private communication.

26. FUNFER, E., Julich. Private communication, October 1966.

27. KÖNEN, L., NOLL, P., SUGITA, K. and WITULSKI, H. Experimental investigations on a 600 kJ theta pinch. First European Conference on Controlled Fusion and Plasma Physics, Munich, October, 1966. (Abstract only)

APPENDIX

ENERGY BALANCE EQUATION

THE MODEL

(i) $T_e + T_i$ independent of radius

(ii) Both temperatures are scalar

(iii) $n_e = n_i$ is independent of radius

(iv) The line density N is constant in time

(v) Flux, φ, is conserved in the plasma

(vi) Pressure balance is satisfied

With these limitations we can write the equation for the balance of energy in 1 cm length of plasma of cross sectional area A_p contained by a magnetic field B which is losing energy at a rate R ergs cm^{-3} sec^{-1}.

$$\frac{d}{dt}\left[3\ nk\ TA_p \right] = -2nk\ T \frac{dA_p}{dt} - RA_p \qquad \ldots (A1)$$

The equation of pressure balance gives us

$$B^2 = \frac{\varphi^2}{A_p^2} + 16\pi nk\ T \qquad \ldots (A2)$$

Since the line density is constant we also have

$$nA_p = N = \text{constant} \qquad \ldots (A3)$$

TIME DEPENDENCE OF TEMPERATURE

Equations (A1), (A2), (A3) can be reduced by elimination of A_p and n to give an equation in T

$$\frac{1}{T}\frac{dT}{dt} = \frac{1}{B}\frac{dB}{dt}\left[\frac{4}{3-\beta} \right] - \frac{R}{B^2} \cdot \frac{16\pi(2-\beta)}{\beta(6-\beta)} \qquad \ldots (A4)$$

where

$$\beta = \frac{2nkT}{B^2/8\pi}$$

[For $\beta = 1$ plasma with no losses this reduces to the normal equation $T \propto B^{4/5}$].

TIME DEPENDENCE OF DIAMAGNETIC SIGNAL

For a uniform plasma described by this model we find that the diamagnetic signal S which can be written as

$$S = \int^{A_p} (B - B_p)\, dA$$

reduces to

$$S = B\, A_p - \varphi \qquad \ldots (A5)$$

Eliminating A_p from this equation one can relate S to the temperature

$$T = \frac{BS}{16\pi Nk}\left[\, 1 + \frac{\varphi}{S + \varphi}\,\right] \qquad \ldots (A6)$$

One can also determine the time variation of S by eliminating A_p from equation (A1) and (A5). One finds

$$\frac{1}{S}\frac{dS}{dt} = -\frac{1}{B}\frac{dB}{dt}\left[\frac{1 + \varphi^2/(S+\varphi)^2}{5 + \varphi^2/(S+\varphi)^2}\right] - \frac{16\pi R}{B^2[5 + \varphi^2/(S+\varphi)^2]} \qquad \ldots (A7)$$

INCLUSION OF THERMAL CONDUCTIVITY IN ENERGY EQUATION

Temperature Equation

To include the effect of thermal conduction we replace RA by $\frac{\partial}{\partial z}\left(AK\frac{\partial T}{\partial z}\right)$ and write K as $\alpha T^{5/2}$ (following Spitzer[11]). If we also write that N, φ are constants in z as well as in time we find

$$\frac{1}{T}\frac{dT}{dt} = \frac{4}{6-\beta}\cdot\frac{dB}{dt} - \frac{16\pi\alpha}{B^2}\cdot\frac{(2-\beta)}{(6-\beta)}\cdot\left[\frac{7}{2}T^{3/2}\left(\frac{\partial T}{\partial z}\right)^2 + T^{5/2}\frac{\partial^2 T}{\partial z^2}\right] \qquad \ldots (A8)$$

If we assume for simplicity

$$T = T_c\,(t)\; T_z\,(z) \qquad \ldots (A9)$$

then both time and spatial parts of equation (A8) can be solved separately.

The boundary conditions of a heat sink are $T = 0$ at $z = L$ and symmetry in the mid plane

$$\left.\frac{dT_z}{dz}\right|_0 = 0$$

can be applied to the spatial part of equation (A8) as follows[25].

$$\frac{7}{2} T_z^{3/2} \left(\frac{dT_z}{dz} \right)^2 + T_z^{5/2} \frac{d^2T_z}{dz^2} = \frac{1}{T_z} \frac{d}{dz} \left(T_z^{7/2} \frac{dT_z}{dz} \right) = C \qquad \ldots (A10)$$

where C is a constant. The first integration gives

$$\left(T_z^{7/2} \frac{dT_z}{dz} \right)^2 = \frac{4}{11} C \left(1 - T_z^{11/2} \right)$$

The constant C can be found with the aid of a definite integral

$$L = \int_0^L dz = \left(\frac{11}{4C} \right)^{1/2} \int_0^1 \frac{T_z^{7/2} \, d T_z}{\sqrt{1 - T_z^{11/2}}}$$

Substituting $x^2 = T_z$

$$LC^{1/2} = 11 \int_0^1 \frac{x^8 dx}{1 - x^{11}} = \sqrt{\frac{\pi}{11}} \frac{\Gamma(9/11)}{\Gamma(\frac{9}{11} + \frac{1}{2})} = 0.684$$

therefore

$$C \approx \frac{0.47}{L^2}$$

The functional form of T_z is complicated and the approximation

$$T_z^{7/2} = 1 - \left(\frac{Z}{L} \right)^2 \qquad \ldots (A11)$$

is sometimes useful.

The equation for the time variation of T_c may now be found by replacing the energy loss term in (A8). i.e.,

$$\frac{1}{T_c} \frac{T_c}{t} = \frac{4}{6 - \beta} \frac{1}{B} \frac{dB}{dt} - \frac{0.468 \; 16\pi\alpha \; (2 - \beta)}{B^2 L^2 \; (6 - \beta)} T_c^{7/2} \qquad \ldots (A12)$$

Diamagnetic Equation

By substituting for R in equation (A7) the alternative form of (A12) may be found representing the behaviour of the diamagnetic signal

$$\frac{1}{S} \frac{dS}{dt} \left[1 + \frac{1}{5} \left(\frac{\varphi}{S + \varphi} \right)^2 \right] = - \frac{1}{5} \frac{1}{B} \frac{dB}{dt} \left[1 + \frac{\varphi}{S + \varphi} \right]$$

$$- \frac{0.47 \times 16\pi\alpha \; B^{3/2} \; S^{5/2}}{5 \; L^2 \; (16\pi N k)^{7/2}} \left(S + \varphi \right) \left(1 + \frac{\varphi}{S + \varphi} \right)^{7/2}$$

$$\ldots (A13)$$

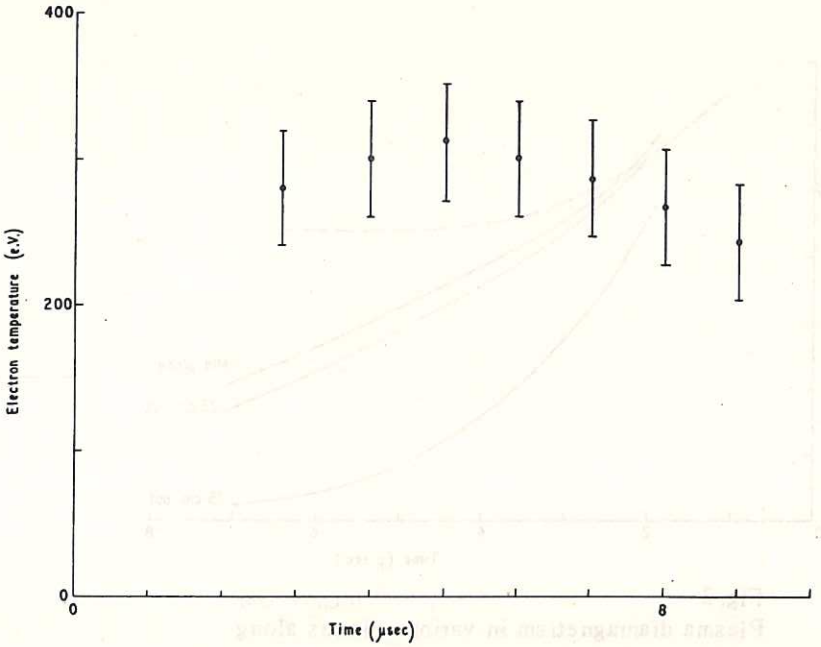

Fig. 1 (CLM-P 124)
Electron temperature measured by the absorber foil technique. Pressure 30 mtorr

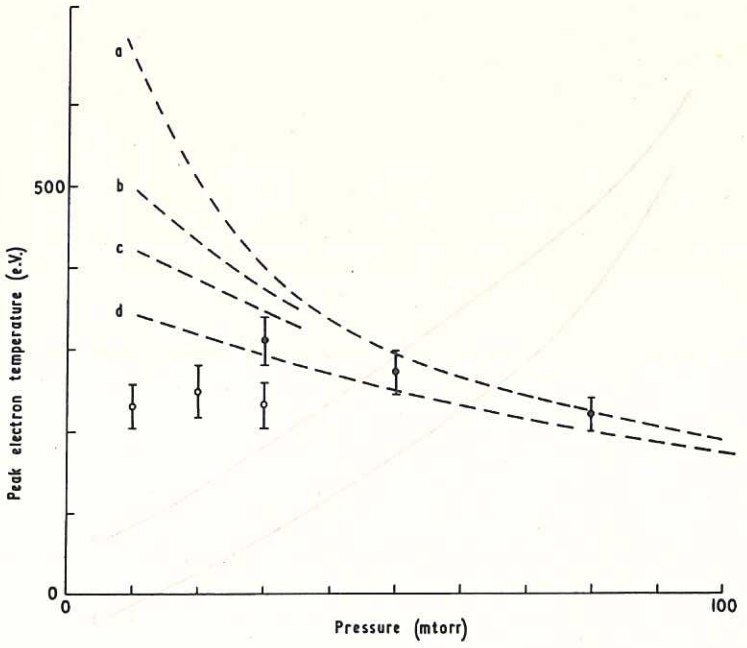

Fig. 2 (CLM-P 124)
Peak electron temperature at various pressures. The full circles represent measurements made with the absorber foil technique and the open circles with grazing incidence spectroscopy. The broken lines are computed from the radial hydromagnetic codes with a thermal conduction loss term
α = transport theory value of coefficient
(a) $0 \times \alpha$ (b) $1 \times \alpha$ (c) $3 \times \alpha$ (d) $10 \times \alpha$

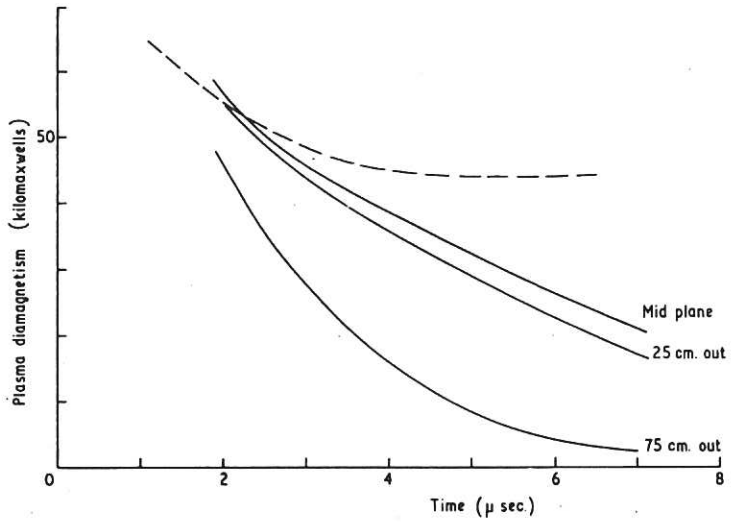

Fig. 3 (CLM-P 124)
Plasma diamagnetism in various planes along the discharge at a pressure of 30 mtorr. The broken curve is that computed for a loss-free plasma by the radial hydromagnetic code

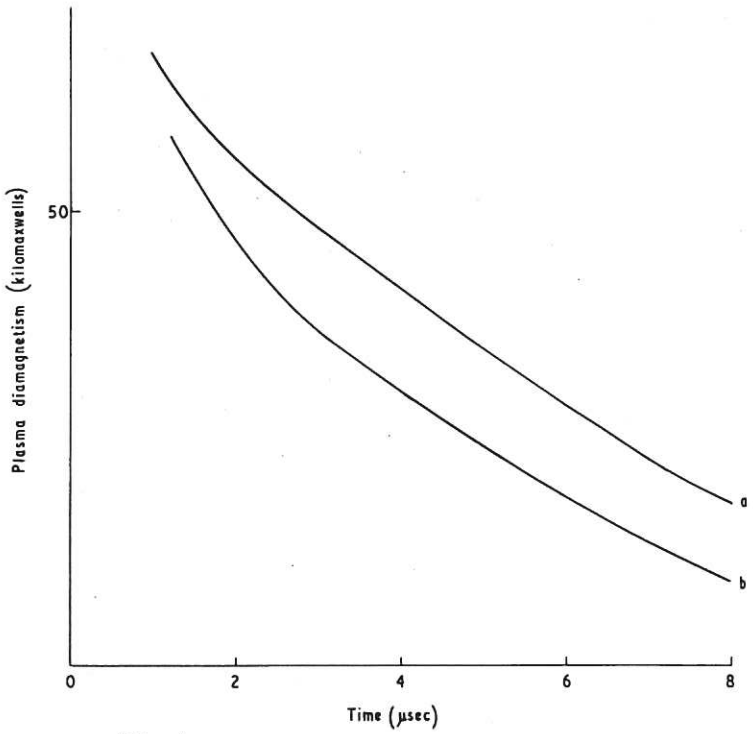

Fig. 4 (CLM-P 124)
Plasma diamagnetism at 30 mtorr pressure with (a) 1.5%; (b) 8% oxygen impurity

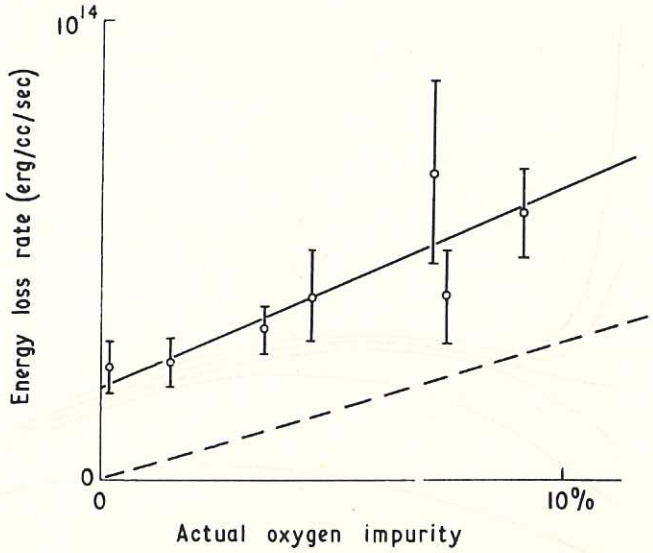

Fig. 5 (CLM-P 124)

Energy loss rate, estimated from the decay of plasma diamagnetism, with various amounts of oxygen contamination. The solid line is the least squares fit of the data to equation (9) and the broken line is the loss rate calculated for OVII and OVIII line radiation with $T_e = 300$ eV and $n_e = 10^{17}$ cm^{-3}

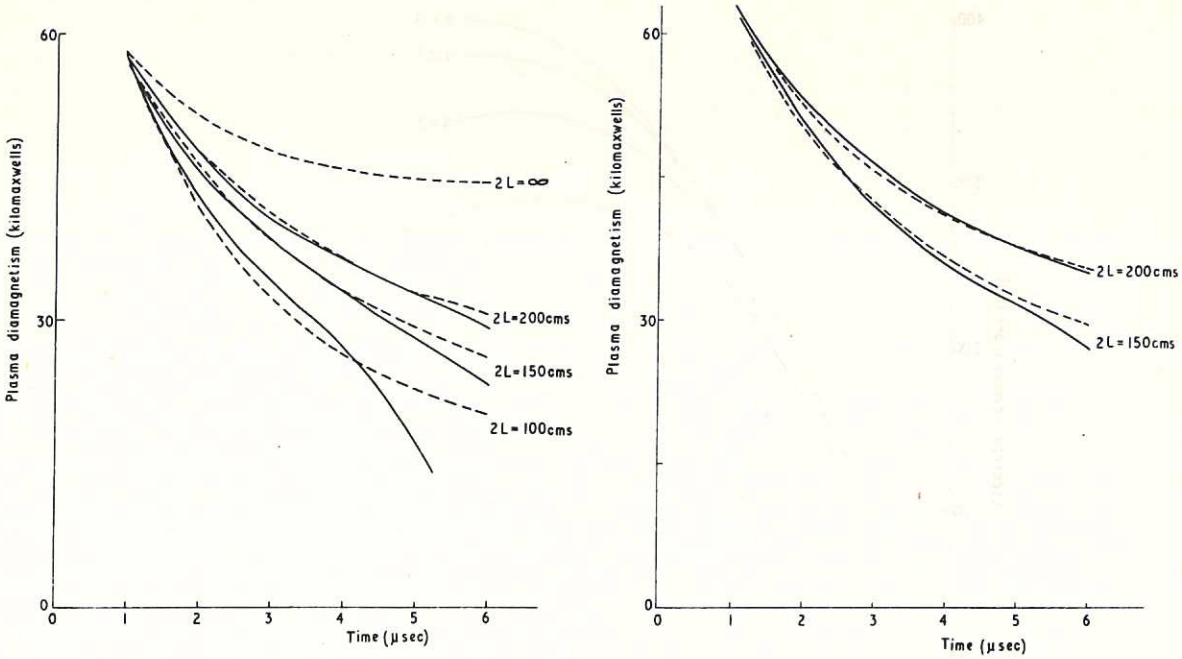

Fig. 6 (CLM-P 124)

Diamagnetism in the mid plane of plasmas in various lengths, 2L, of theta pinch coil. Initial pressures (a) 43 mtorr, and (b) 61 mtorr. The broken lines are computed using the model of thermal conduction cooling

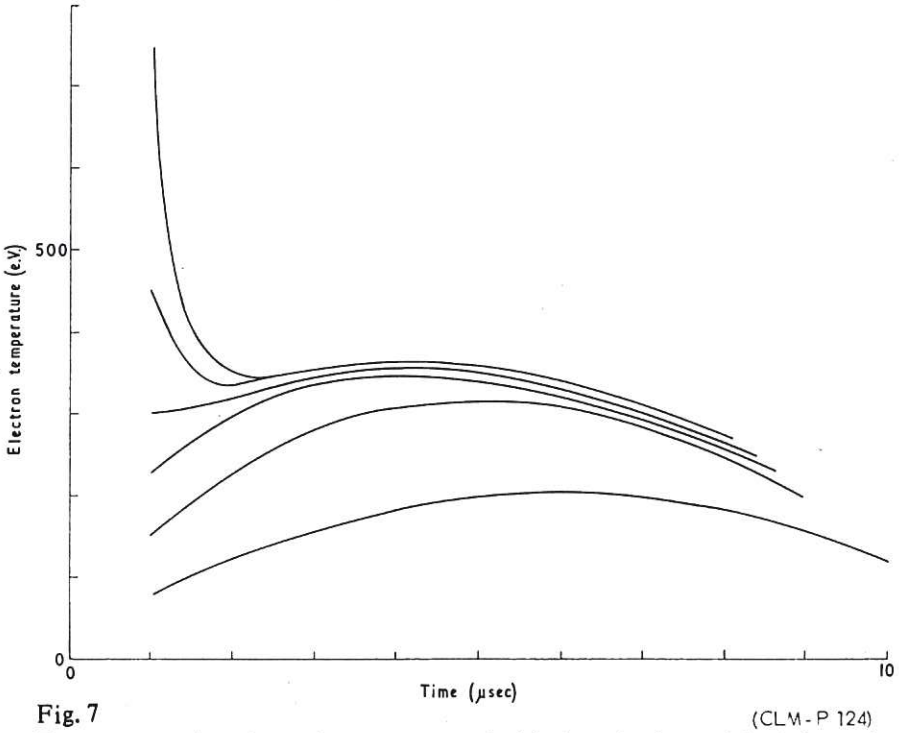

Fig. 7 (CLM-P 124)

Temperature-time dependence computed with the simple model of thermal conduction cooling. Various initial temperatures are assumed

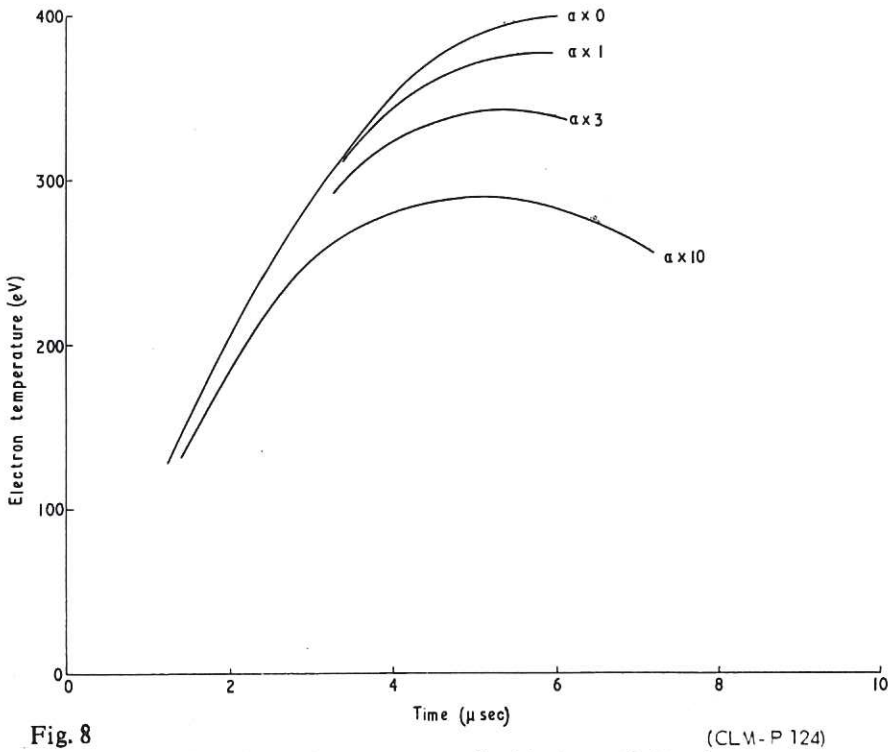

Fig. 8 (CLM-P 124)

Temperature-time dependence computed with the radial hydromagnetic code including an energy loss term to simulate thermal conduction. Initial pressure 30 mtorr

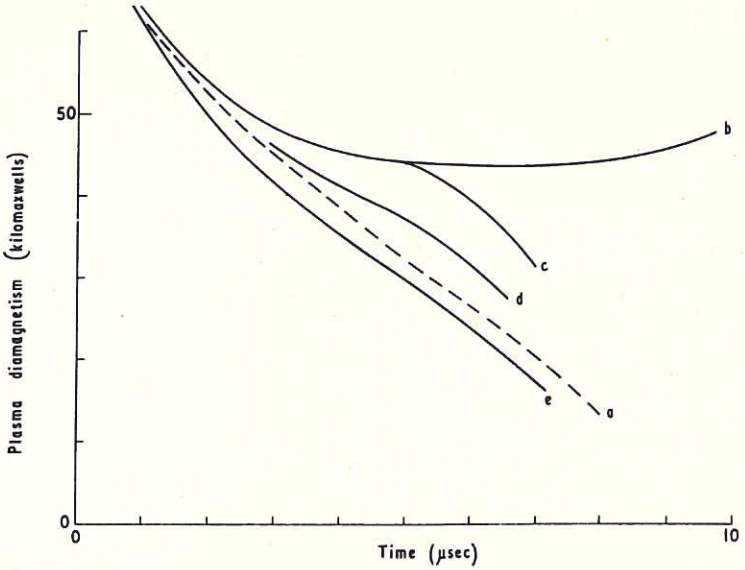

Fig. 9 (CLM-P 124)

Plasma diamagnetism in the mid-plane. Initial pressure 30 mtorr. (a) experimental result; (b) computed with radial code, $0 \times a$; (c) computed with axial code, $0 \times a$; (d) as (c) but $4 \times a$; (e) as (c) but $10 \times a$

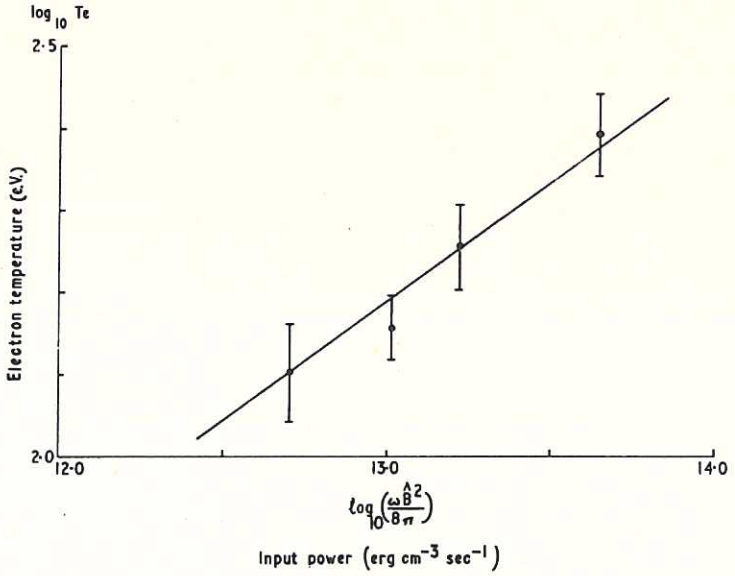

Fig. 10 (CLM-P 124)

Variation of electron temperature with input power. Measurements made with the grazing incidence spectrometer at 20 mtorr pressure.